



Study on Characteristics of Multilayer Biosensor*

HE Li-Dong¹⁾, LI Jian-Ping^{1)**}, WEI Bi-Qian¹⁾, WEN Jian-Ming¹⁾, LIU Hao²⁾, MA Ji-Jie¹⁾,
 HU Yi-Li¹⁾, ZHANG Yu¹⁾, WAN Nen¹⁾, LI Ning^{3)**}

¹⁾College of Engineering, Zhejiang Normal University, Jinhua 321004, China;

²⁾College of Information Science and Engineering, Jiaying College, Jiaying 314000, China;

³⁾Hangzhou Innovation Institute, Beihang University, Hangzhou 310051, China)

Abstract Objective Biosensors with multilayer biomedica are widely applied in various fields, and quantitative characterization of biosensors is still a problem for the development of sensors. This study is to quantitatively characterize the electrical properties of multilayer biomedica. **Methods** Combined with conformal mapping theory, the quantitative characteristics of biosensors are explored based on electrical impedance spectroscopy for clarifying the law of influence on impedance, and this study provides a basic theory for the characterization of biosensors. The impedance (Z) of each biomedica layer is extracted, and the simulation and calculation are executed to study the correctness. **Results** An experimental system has been established, results show that the impedance (Z) of the detection area continues to rise from the frequency (f) = 0.1 MHz to f =50.0 MHz in the coating process. This trend is explained that the solution in the original detection area is covered by the coating of biological medium with different dielectric properties, resulting in a decrease in the conductivity of the detection area and an increase in the impedance. Theoretical calculation results and simulation results show a great agreement with experimental results. **Conclusion** This study confirms that the multilayer biosensors are able to be quantitatively characterized based on electrical impedance spectroscopy and conformal mapping, which has certain practical value for the further development of biosensors.

Key words biosensor, multilayer biomedica, electrical impedance spectroscopy, conformal mapping, impedance

DOI: 10.16476/j.pibb.2022.0305

Biosensors with high detection sensitivity, low production cost and convenient operation are widely applied in various fields, such as ecological environment monitoring^[1-5], food safety detection^[6-10], medical disease diagnosis^[11-13] and bioengineering^[14]. With the rapid development of biosensors, the requirements for structure design and performance of biosensors have been increased continuously by research scholars. The selection of electrodes, the modification process and the improvement of materials are the keys to achieve stable signal conversion and transmission. For example, interdigital electrodes are extensively used in biosensors due to its unique comb-like structure, high sensitivity and fast response speed. Functionalized biosensors were used to detect the concentration of acquired immune deficiency syndrome (AIDS)-killing anaphylaxis^[15-16], and micro biosensors were used for *in situ* non-invasive detection of glucose in sweat^[17]. There are already numerous researches on biosensors in the past decades all over the world. It is seen that biosensors

have important function in the aspect of rapid disease diagnosis, life quality protection and life safety maintenance.

Biosensors are mainly composed of planar electrodes which has been modified one or more layers of polymers on the surface by physical or chemical means. Combined with electrical impedance spectroscopy, the output signals are obtained by sweeping frequency under the electrode polarization band to illustrate the change caused by the adsorption of the medium. Existing researches optimize and

* This work was supported by grants from The National Natural Science Foundation of China (52105564), the Natural Science Foundation of Zhejiang Province (LGF20E050001), Zhejiang Provincial Key Research and Development Project of China (2021C01181), and Hangzhou Innovation Institute, Beihang University (2020-Y1-A-028).

** Corresponding author.

LI Jian-Ping. Tel: 86-579-82288627, E-mail: lijip@zjnu.cn

LI Ning. Tel: 86-17398065970, E-mail: liningjlu@163.com

Received: June 28, 2022 Accepted: August 1, 2022

theoretically verify the structural parameters of biosensors, which are widely promoted in substance detection. Rui *et al.* [18] proposed the analytical expression of the periodic interdigital electrode capacitive sensor, and studied the capacitance characteristics of the multilayer dielectric layer and the interdigital electrode parameters. Wang *et al.* [19] calculated the planar capacitance characteristics in the multilayer dielectric structure which was simulated and verified, and the capacitance of the interdigital electrodes with different parameters of the dielectric structure was compared. Ibrahim *et al.* [20] studied the influence of electrode geometric parameters on impedance spectrum to optimize three-dimensional biomedium-loaded sensors. Biosensors with improved performance have played a very important role in various fields. Rajibur *et al.* [21] designed and developed a taste sensor array based on the interdigital capacitor, which was combined with various tastes by spin-coating lipids. This method has the advantages of real-time monitoring capability and high sensitivity through voltage changes caused by different tastes and lipid binding. Jung *et al.* [22] developed a capacitive biosensor with nano-island structure interdigital electrodes for antigen-antibody interaction. In recent years, the research on the optical/electrical properties of multi-layer coatings has continued to deepen, but the current research mostly stays on the qualitative research of the multi-layer uniform biological medium structure. The research and theoretical exploration of the quantitative characteristics of the multi-layered biological medium need to be further explored.

In this study, characteristics of multilayer biological medium based on the electrical impedance spectroscopy has been explored. Combined with the method of conformal mapping, the plane electrode is converted into a parallel electrode, which expands the original theory. The simulation and calculation of multilayer model are executed. An experimental system has been established and the results show that impedance increases with the modifying process of the medium, and the theoretical calculation results and simulation results show a great agreement with the experimental results. This study presents a method for quantifying the electrical impedance properties of multilayer biomedium based on conformal mapping and electrical impedance spectroscopy.

1 Materials and methods

1.1 System

Figure 1a shows the detection system for multilayer biomedium electrical impedance spectrum characteristic, and it is mainly composed of a detection container, an impedance analyzer, a dedicated impedance fixture device and a PC. The detection container is consisted of periodic interdigitated electrodes which is made of gold by lithography and polymethyl methacrylate (PMMA) cavity, and the detailed dimensions are shown in Figure 1b: the electrode line width (W)=100 μm , the line spacing (D)=100 μm , and the number of electrodes (N)=20. Figure 1c shows the multilayer biomedium structure detected in the experiment. A bottom-up layers are the electrode layer, polydopamine (PDA) layer, bovine serum albumin (BSA) layer and sodium chloride (NaCl) solution layer. The detection container is connected to the data detection terminal of the impedance analyzer (Hyoki, IM7581) through a special impedance fixture device (Hyoki, IM9200). The impedance analyzer applies a current (I)=0.001 A to the detection container and sweeps the frequency (f) from $f=0.1$ MHz to $f=300.0$ MHz which used to measure the electrical impedance spectrum characteristics of multilayer biomedium. The PC is connected to the data transmission port of the impedance analyzer for data processing and storage.

1.2 Theoretical analysis

The equivalent circuit of periodic interdigitated electrodes is shown in Figure 2. According to earlier studies [18, 23], C_1^* presents the half complex capacitance of an inner electrode relative to the ground potential, and C_E^* presents the complex capacitance of an outer electrode relative to the ground plane beside to it. The total complex capacitance (C^*) will be calculated by the method of conformal mapping:

$$\varepsilon_m^* = \varepsilon_m - j \frac{\sigma_m}{\omega \varepsilon_0} \quad (1)$$

$$C_1^* = \varepsilon_0 \cdot \varepsilon_m^* \cdot L \cdot \frac{K(k_1)}{K(k_1')} \quad (2)$$

$$C_E^* = \varepsilon_0 \cdot \varepsilon_m^* \cdot L \cdot \frac{K(k_E)}{K(k_E')} \quad (3)$$

$$C^* = (N - 3) \frac{C_1^*}{2} + \frac{2C_1^*C_E^*}{C_1^* + C_E^*}, N \geq 3 \quad (4)$$

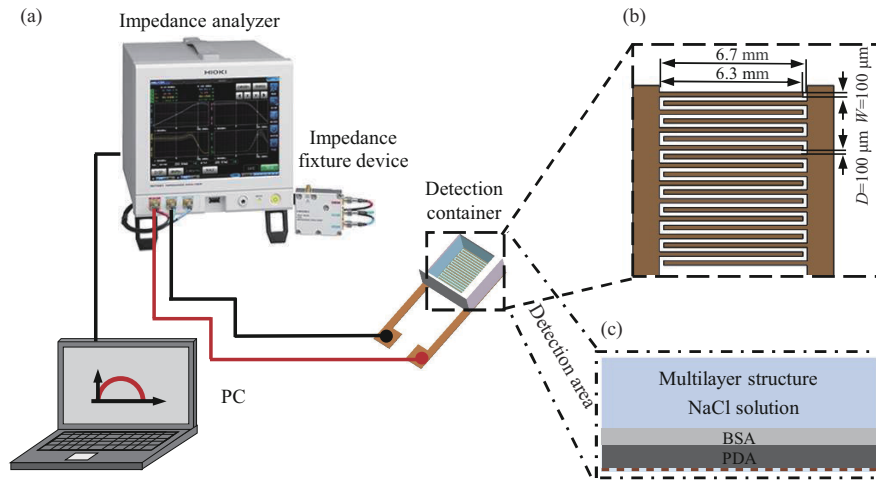


Fig. 1 Detection device

(a) Detection system; (b) periodic interdigital electrode; (c) multilayer biological medium structure.

where ϵ_0 is the permittivity of air, ϵ_m is the permittivity of the medium, σ_m is the conductivity of the medium, ϵ_m^* is the complex permittivity of the medium, L is the electrode finger length, N is the number of electrodes, and $K(k)$ is complete elliptic integrals of the first kind,

k_1 and k_E are the elliptic modulus of the inner electrode and the outer electrode, respectively, k'_1 and k'_E are the complementary modulus of the inner electrode and the outer electrode, respectively.

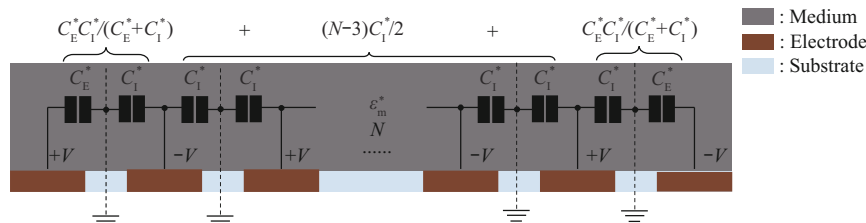


Fig. 2 Equivalent circuit diagram of periodic interdigital electrode

According to the impedance calculation formula^[24-27], it can be obtained:

$$Z^* = \frac{1}{j\omega C^*} = \frac{1}{j2\pi f C^*} \quad (5)$$

where Z^* is the impedance, j is the imaginary unit, ω is the angular frequency, and f is the frequency.

The schematic cross-section of the periodic interdigital electrode is shown in Figure 3. Figure 3a shows a schematic cross-sectional view of a single-layer dielectric. T_s and ϵ_s are the thickness and dielectric constant of the solution dielectric layer, respectively. Figure 3b shows a schematic cross-sectional view of a multilayer dielectric. T_b and ϵ_b are

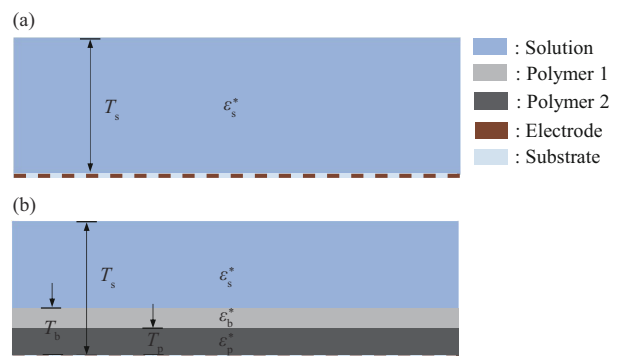


Fig. 3 Cross section diagram of periodic interdigital electrode detection

(a) Monolayer biological medium; (b) multilayer biological medium.

the thickness and dielectric constant of the polymer 1 dielectric layer, respectively; T_p and ϵ_p are the thickness and dielectric constant of the polymer 2 dielectric layer, respectively. The electrode width is $W=100\ \mu\text{m}$, the electrode spacing is $D=100\ \mu\text{m}$, the number of electrodes is $N=20$, and the electrodes are embedded in the substrate so the thickness is negligible.

The impedance of a single-layer medium can be obtained according to equations (1)–(5):

$$\epsilon_s^* = \epsilon_s - j \frac{\sigma_s}{\omega \epsilon_0} \quad (6)$$

$$C_{Is}^* = \epsilon_0 \cdot \epsilon_s^* \cdot L \cdot \frac{K(k_{Is})}{K(k'_{Is})} \quad (7)$$

$$C_{Es}^* = \epsilon_0 \cdot \epsilon_s^* \cdot L \cdot \frac{K(k_{Es})}{K(k'_{Es})} \quad (8)$$

$$C_s^* = \frac{17C_{Is}^*}{2} + \frac{2C_{Is}^*C_{Es}^*}{C_{Is}^* + C_{Es}^*} \quad (9)$$

$$Z_s^* = \frac{1}{j\omega C_s^*} = \frac{1}{j2\pi f C_s^*} \quad (10)$$

where ϵ_s^* is the complex permittivity of the solution, σ_s is the electrical conductivity of the solution, C_{Is}^* , C_{Es}^* are the complex capacitances of the internal and external electrodes of the solution, C_s^* is the complex capacitance of the solution, Z_s^* is the impedance of the solution, k_{Is} , k_{Es} are the elliptic moduli of the inner and outer electrodes of the solution, respectively, and k_{Is}' and k_{Es}' are complementary moduli.

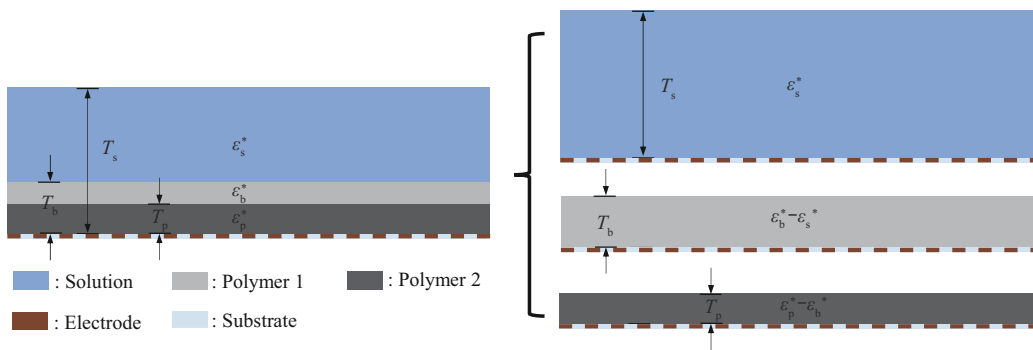


Fig. 4 Equivalent diagram of multilayer biological medium

2 Results and discussion

2.1 Theoretical calculation results

The theoretical formula is introduced in MatLab to verify the the feasibility of the experiment. During

As shown in Figure 4, the multilayer biological medium is approximately divided into the sum of multiple single-layer biological mediums supported by recent research. The formula based on equations (1)–(5) for impedance which are described by:

$$\epsilon_i^* = \epsilon_i - j \frac{\sigma_i}{\omega \epsilon_0}, i = b, p, s \quad (11)$$

$$C_{li}^* = \epsilon_0 \cdot \epsilon_i^* \cdot L \cdot \frac{K(k_{li})}{K(k'_{li})}, i = b, p, s \quad (12)$$

$$C_{Ei}^* = \epsilon_0 \cdot \epsilon_i^* \cdot L \cdot \frac{K(k_{Ei})}{K(k'_{Ei})}, i = b, p, s \quad (13)$$

$$C_i^* = \frac{17C_{li}^*}{2} + \frac{2C_{li}^*C_{Ei}^*}{C_{li}^* + C_{Ei}^*}, i = b, p, s \quad (14)$$

$$C_t^* = \sum_{i=b,p,s} C_i^* \quad (15)$$

$$Z_t^* = \frac{1}{j\omega C_t^*} = \frac{1}{j2\pi f C_t^*} \quad (16)$$

where ϵ_i^* and σ_i are the complex permittivity and conductivity of bovine serum albumin, polydopamine and the solution, respectively; C_{li}^* and C_{Ei}^* are the complex capacitance of BSA, polydopamine and the inner and outer electrodes of the solution, respectively; C_i^* is the complex capacitance of bovine serum albumin (BSA), polydopamine and the solution, C_t^* is the total complex capacitance, Z_t^* is the total impedance, k_{li} and k_{Ei} are the elliptic modulus of bovine serum albumin, polydopamine and the inner and outer electrodes of the solution, respectively; k_{li}' and k_{Ei}' are complementary moduli.

the process of parameter setting, since the permittivity and conductivity of each biological medium are related to the electrical impedance characteristics, the parameters are estimated and set in the theoretical calculation process ($\epsilon_s > \epsilon_b > \epsilon_p$, $\sigma_s > \sigma_b > \sigma_p$).

The numerical results are shown in Figure 5 under the condition that the input frequency is swept from 0.1 MHz to 300.0 MHz. Figure 5 describes that after the electrode is coated with PDA, its arc is significantly larger than the arc without coating effect, which means the impedance value of the electrode detection area indicates an upward trend; further, after BSA coating, its arc is slightly enlarged compared

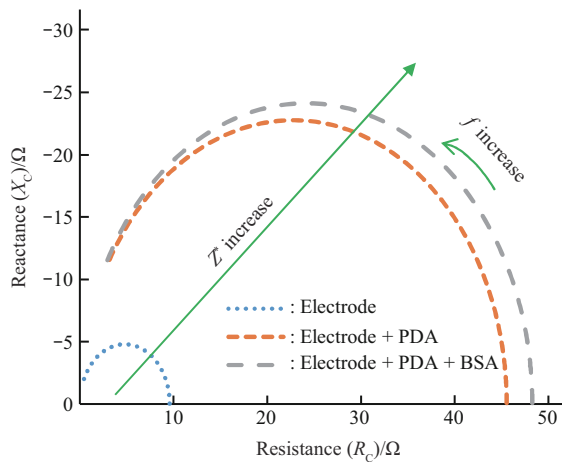


Fig. 5 Theoretical calculation results

with that under PDA coating, which also displays that the impedance value of the electrode detection area presents an upward trend. Overall, the theoretical calculation results show an upward trend.

2.2 Simulation results

The feasibility of experiments are verified by theoretical analysis. As shown in Figure 6, the multi-physics finite element analysis, grasping the characteristics, parameters and functions of each module systematically and judging the practicability of the system, is applied to explore the influence of the impedance characteristics. The finite element simulation structure is simplified, three pairs of plane electrodes are arranged, the interval is kept same, and the input current is 10 mA. The sweep frequency range is 0.1 MHz to 800.0 MHz for observing the test trend visually. In the multi-physics finite element analysis process, the multilayer biological structure is drawn according to the theoretical structure which is assigned different permittivity and conductivity ($\epsilon_s > \epsilon_b > \epsilon_p$, $\sigma_s > \sigma_b > \sigma_p$). Figure 6a-c are the potential distribution diagrams of single-layer, double-layer,

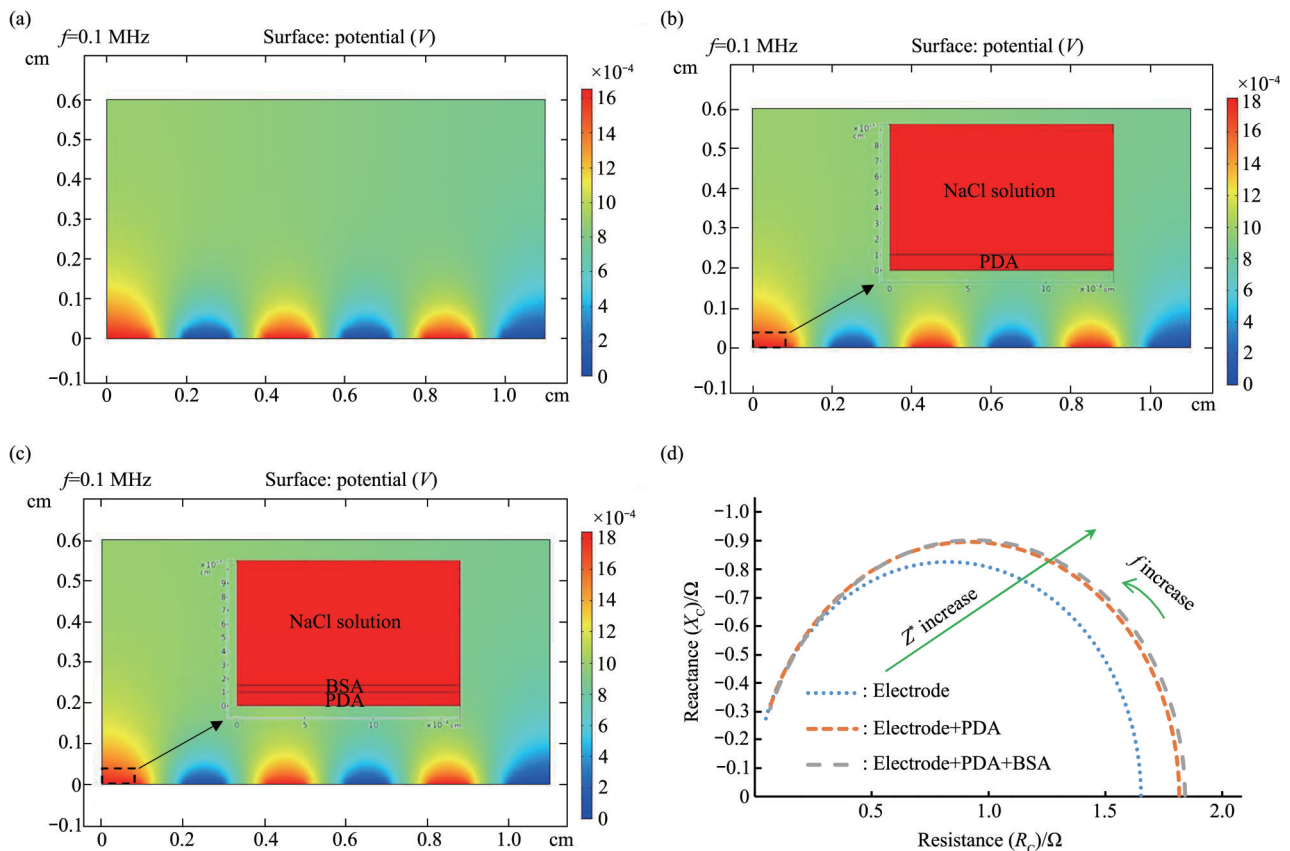


Fig. 6 Finite element analysis and results

(a) Electrode potential distribution diagram; (b) Electrode+PDA potential distribution diagram; (c) Electrode+PDA+BSA potential distribution diagram. (d) Simulation results.

and three-layer simulated electrode modification. Figure 6d reveals a Nyquist plot of the impedance characteristics of a multilayer dielectric obtained from a multiphysics finite element simulation. It will be explained that, when the electrode is modified by multilayer biological medium, the semicircle of the Nyquist plot becomes larger. In general, there is an increasing trend consistent with the theoretical calculation results in Figure 5.

2.3 Experiment results

Figure 7 shows the impedance-frequency characteristic curve of the modified multilayer biological medium. Especially, Figure 7a indicates that, impedance changes from frequency (f)=0.1 MHz to 50.0 MHz under the condition of different medium modification. Figure 7b illustrates impedance at frequency (f) =0.1 MHz to f =1.0 MHz which magnified from Figure 7a is changed. Seriously, the modification of the electrode by the multilayer biological medium causes the impedance change to be

more obvious. There are described that, when the frequency is swept exponentially from 0.1 MHz to 50.0 MHz, the impedance in the detection area shows a slow decreasing trend which remains the same under different biological medium coating. To elaborate further, when the frequency is kept at 1.0 MHz, the impedance of the uncoating electrode detection area is around 45.44 Ω , and the impedance value of the electrode detection area after coating by PDA is about 48.01 Ω , when the electrode after coating with BSA, the impedance value of the detection area is approximately 48.75 Ω , which confirms that the coating of the biological medium has an effect on the impedance characteristics; meanwhile, when the frequency is kept at 50.0 MHz, the impedance of the electrode detection area before and after coating remains between 19.40 Ω and 19.90 Ω , confirming that the coating of biological medium has little effect on the impedance characteristics after this frequency.

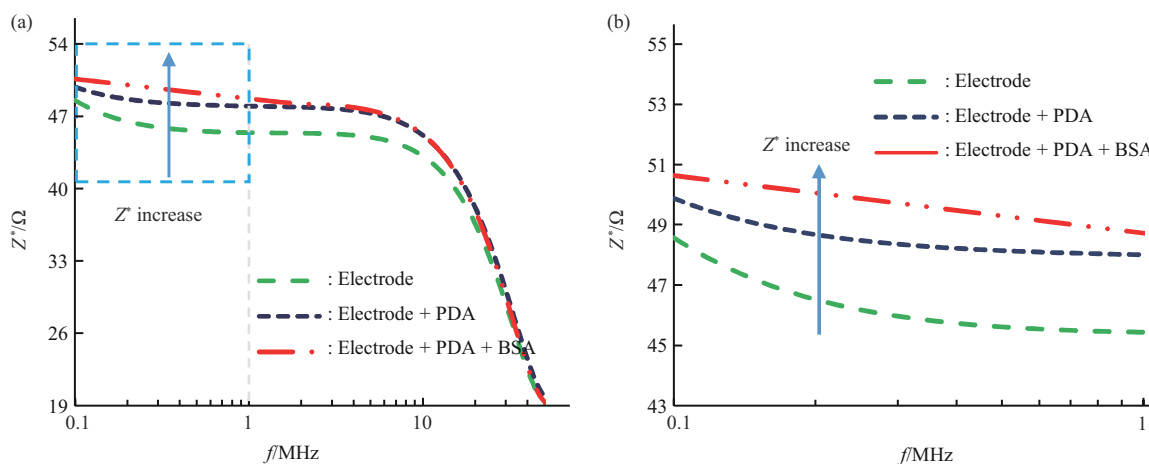


Fig. 7 Impedance frequency characteristic curve of modified electrode

(a) 0.1 MHz to 50.0 MHz; (b) 0.1 MHz to 1.0 MHz.

As shown in above figures, the biosensor is more sensitive at relatively low frequencies. The reactance has a positive and negative difference between the inductive reactance and the capacitive reactance during the detection process. In this study, the reactance takes the negative value section due to the inductive reactance that generally influenced by the electrodes and wires, which will affect the experimental data. Therefore, the frequency is selected at f =0.1 MHz to f =35.0 MHz as shown in Figure 8. The electrode polarization occurs at the

interface between the liquid and the electrode surface. During the experiment, the data collected by the impedance analyzer not only includes the experimental sample, but also is affected by the geometry of the detection device and its own parasitic impedance and electrode polarization, which will not be analyzed in detail here; the semicircular arc segment is named the interface polarization occurs at the interface of different phases. From the analysis of the experimental results, the arc of the Nyquist curve expands outward, and the impedance value presents a

gradual upward trend with the continuous coating of the biological medium on the electrode surface. This trend is explained by the fact that the solution in the original detection area is covered by the coating of biological medium with different dielectric properties, resulting in a decrease in the conductivity of the detection area and an increase in the impedance. Overall, although the experimental results that compared with the theoretical calculation results and the simulation results may have errors due to the real structure size, dielectric parameter setting of materials, coating process and other problems, the theoretical calculation results and the simulation results are in good agreement with the experimental results as shown in Figure 5, 6, which explains the accuracy of the experiments in a certain extent.

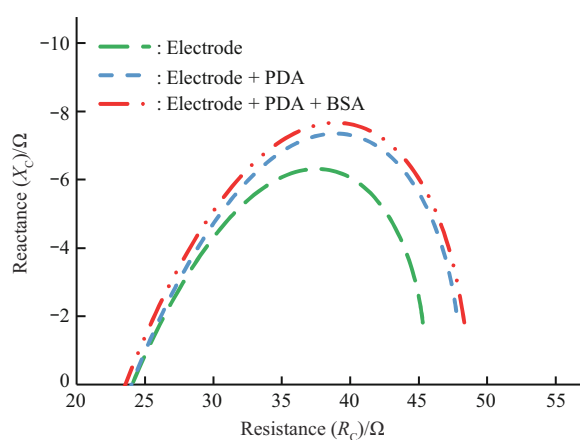


Fig. 8 Nyquist curve of modified electrode

3 Conclusion

In this study, characteristics of multilayer biological medium based on the electrical impedance spectroscopy has been explored. Combined with the method of conformal mapping, the plane electrode is converted into a parallel electrode, which expands the original theory. The experimental results illustrated that after immobilization of the biological medium layer, the electrical impedance in the detection area continues to rise from frequency (f)=0.1 MHz to f =50.0 MHz. At frequency (f)=1.0 MHz, the electrode experienced three stages (bare electrode, PDA and BSA), and the detection area results were 45.44 Ω , 48.01 Ω , and 48.75 Ω , respectively. The impedance value of the overall detection area shows an upward

trend in a certain frequency range with the coating of the biological medium layer. The theoretical calculation results and simulation results display a great consistent with the experimental results, which demonstrate the correctness of this way. This study confirms that the impedance spectrum characteristics of multilayer biological medium is able to be quantified by the electrical impedance spectroscopy and conformal mapping, which has certain pragmatic value for the research and the development of biosensors.

References

- [1] Kroger S, Piletsky S, Turner A. Biosensors for marine pollution research, monitoring and control. *Mar Pollut Bull*, 2002, **45**(1-12): 24-34
- [2] Aracic S, Manna S, Petrovski S, *et al.* Innovative biological approaches for monitoring and improving water quality. *Front Microbiol*, 2015, **6**: 826
- [3] Li Y, Ren Z X, Qi R L, *et al.* Detection of total nitrogen based on electrochemical sensor. *Chines J Anal Chem*, 2020, **48**(3): 316-322
- [4] Ramirez-Priego P, Estévez M C, Díaz-Luisravelo H J, *et al.* Real-time monitoring of fenitrothion in water samples using a silicon nanophotonic biosensor. *Anal Chim Acta*, 2021, **1152**(3): 338276
- [5] Dey S, Baba S A, Bhatt A, *et al.* Transcription factor based whole-cell biosensor for specific and sensitive detection of sodium dodecyl sulfate. *Biosens Bioelectron*, 2020, **170**: 112659
- [6] Lü M, Liu Y, Geng J H, *et al.* Engineering nanomaterials-based biosensors for food safety detection. *Biosens Bioelectron*, 2018, **106**: 122-128
- [7] Huang F C, Zhang Y C, Lin J H, *et al.* Biosensors coupled with signal amplification technology for the detection of pathogenic bacteria: a review. *Biosensors (Basel)*, 2021, **11**(6): 190
- [8] Griesche C, Baeumner A J. Biosensors to support sustainable agriculture and food safety. *Trend Anal Chem*, 2020, **128**: 115906
- [9] Chauhan N M, Washe A P, Minota T. Fungal infection and aflatoxin contamination in maize collected from Gedeo zone, Ethiopia. *Springerplus*, 2016, **5**(1): 753
- [10] Wang Y X, Ye Z Z, Si C Y, *et al.* Monitoring of *Escherichia coli* O157: H7 in food samples using lectin based surface plasmon resonance biosensor. *Food Chem*, 2013, **136**(3-4): 1303-1308
- [11] Küilerich-Pedersen K, Poulsen C R, Jain T, *et al.* Polymer based biosensor for rapid electrochemical detection of virus infection of human cells. *Biosens Bioelectron*, 2011, **28**: 386-392
- [12] El-Safty S A, Shenashen M A. Nanoscale dynamic chemical, biological sensor material designs for control monitoring and early detection of advanced diseases. *Mater Today Bio*, 2020, **5**: 100044
- [13] Lu Y, Zhou Q Q, Xu L. Non-invasive electrochemical biosensors for TNF-alpha cytokines detection in body fluids. *Front Bioeng Biotech*, 2021, **9**: 701045

- [14] Goers L, Ainsworth C, Goey C H, *et al.* Whole - cell *Escherichia coli* lactate biosensor for monitoring mammalian cell cultures during biopharmaceutical production. *Biotechnol Bioeng*, 2017, **114**(6): 1290-1300
- [15] Chan J X, Soraya G V, Craig L, *et al.* Rapid detection of HLA-B*57:01-expressing cells using a label-free interdigitated electrode biosensor platform for prevention of abacavir hypersensitivity in HIV treatment. *Sensors (Basel)*, 2019, **19**(16): 3543
- [16] Soraya G V, Chan J, Nguyen T C, *et al.* An interdigitated electrode biosensor platform for rapid HLA-B*15:02 genotyping for prevention of drug hypersensitivity. *Biosens Bioelectron*, 2018, **111**: 174-183
- [17] Han J Y, Li M J, Li H J, *et al.* Pt-poly(L-lactic acid) microelectrode-based microsensor for *in situ* glucose detection in sweat. *Biosens Bioelectron*, 2020, **170**: 11267
- [18] Rui I, Dias C J. Analytical evaluation of the interdigital electrodes capacitance for a multi-layered structure. *Sensor Actuat A Phys*, 2004, **112**(2-3): 291-301
- [19] 王骏. 多层介质结构中叉指电极的平面电容特性. *山东工业技术*, 2017, **17**(2): 146
Wang J. *Shandong Ind Technol*, 2017, **17**(2): 146
- [20] Ibrahim M, Claudel J, Kourtiche D, *et al.* Geometric parameters optimization of planar interdigitated electrodes for bioimpedance spectroscopy. *J Elec Bioimpeda*, 2013, **4**(1): 13-22
- [21] Rajibur K M, Kang S W. Highly sensitive multi-channel IDC sensor array for low concentration taste detection. *Sensors (Basel)*, 2015, **15**(6): 13201-13221
- [22] Jung H W, Chang Y W, Lee G Y, *et al.* A capacitive biosensor based on an interdigitated electrode with nanoislands. *Anal Chim Acta*, 2014, **844**: 27-34
- [23] 赵孔双. 介电谱方法及应用. 北京: 化学工业出版社, 2008: 3-16
Zhao K S. *Dielectric Spectroscopy Methods and Applications*. Beijing: Chemical Industry Press, 2008: 3-16
- [24] Bao H L, Li J M, Wen J M, *et al.* Quantitative evaluation of burn injuries based on electrical impedance spectroscopy of blood with a seven-parameter equivalent circuit. *Sensors-Basel*, 2021, **21**(4): 149
- [25] Li J P, Wan N, Wen J M, *et al.* Quantitative detection and evaluation of thrombus formation based on electrical impedance spectroscopy. *Biosens Bioelectron*, 2019, **141**: 111437
- [26] Li J P, Sapkota A, Kikuchi D, *et al.* Red blood cells aggregability measurement of coagulating blood in extracorporeal circulation system with multiple-frequency electrical impedance spectroscopy. *Biosens Bioelectron*, 2018, **112**: 79-85
- [27] Li J P, Kikuchi D, Sapkota A, *et al.* Quantitative evaluation of electrical parameters influenced by blood flow rate with multiple-frequency measurement based on modified Hanai mixture formula. *Sensors Actuat B Chem*, 2018, **268**: 7-14

多层生物介质传感器的特性研究*

何立栋¹⁾ 李建平^{1)**} 魏碧倩¹⁾ 温建明¹⁾ 刘浩²⁾ 马继杰¹⁾ 胡意立¹⁾
张昱¹⁾ 万嫩¹⁾ 李柠^{3)**}

¹⁾ 浙江师范大学工学院, 金华 321004;

²⁾ 嘉兴学院信息科学与工程学院, 嘉兴 314000; ³⁾ 北京航空航天大学杭州创新研究院, 杭州 310051)

摘要 **目的** 多层生物介质的生物传感器被广泛应用于各大领域, 其检测特性对于传感器优劣的评估尤为重要。本文目的在于量化表征多层生物介质的电学特征。**方法** 基于生物电阻抗谱技术来探究多层生物介质的电化学阻抗谱特性, 并结合保角映射的方法来量化表征多层生物介质, 阐明其对阻抗的影响规律, 继而为生物传感器的研制与开发提供理论基础。有效提取各生物介质层修饰后电阻抗参数 (Z'), 从而量化表征多层生物介质层的电阻抗谱特性。**结果** 对多层模型进行了理论计算并构建了相关试验测试系统, 研究表明, 随着生物介质层的逐步修饰, 检测区域电阻抗参数 (Z') 在 $f=0.1\sim 50$ MHz 下持续上升, 理论计算结果趋势与试验结果趋势较好吻合, 论证了此理论计算方法的正确性。**结论** 本文证实了可根据生物电阻抗谱和保角映射方法量化表征多层生物介质的电阻抗谱特性, 对生物传感器的研制与开发有一定的实用价值。

关键词 生物传感器, 多层生物介质, 生物电阻抗谱, 保角映射, 阻抗

中图分类号 R2-0

DOI: 10.16476/j.pibb.2022.0305

* 国家自然科学基金 (52105564), 浙江省自然科学基金 (LGF20E050001), 浙江省重点研究开发项目 (2021C01181) 和北航杭州创新研究院钱江实验室开放基金 (2020-Y1-A-028) 资助项目。

** 通讯联系人。

李建平 Tel: 0579-82288627, E-mail: lijn@zjnu.cn

李柠 Tel: 17398065970, E-mail: linn@163.com

收稿日期: 2022-06-28, 接受日期: 2022-08-01